Contents lists available at ScienceDirect

ISA Transactions

journal homepage: www.elsevier.com/locate/isatrans

Research article

Diffusion control for a tempered anomalous diffusion system using fractional-order PI controllers

Juan Chen [a,b,*], Bo Zhuang [a,b], YangQuan Chen [c], Baotong Cui [a,b]

[a] Key Laboratory of Advanced Process Control for Light Industry (Ministry of Education), Jiangnan University, Wuxi 214122, PR China
[b] School of IoT Engineering, Jiangnan University, Wuxi 214122, PR China
[c] Mechatronics, Embedded Systems and Automation Lab, University of California, Merced, CA 95343, USA

ARTICLE INFO

Article history:
Received 29 August 2016
Received in revised form
20 March 2017
Accepted 7 April 2017

Keywords:
Fractional-order PI controller
Tempered anomalous diffusion process
FO-Diff-MAS2D-FOPI
FOPI-based CVT alogrithm

ABSTRACT

This paper is concerned with diffusion control problem of a tempered anomalous diffusion system based on fractional-order PI controllers. The contribution of this paper is to introduce fractional-order PI controllers into the tempered anomalous diffusion system for mobile actuators motion and spraying control. For the proposed control force, convergence analysis of the system described by mobile actuator dynamical equations is presented based on Lyapunov stability arguments. Moreover, a new Centroidal Voronoi Tessellation (CVT) algorithm based on fractional-order PI controllers, henceforth called FOPI-based CVT algorithm, is provided together with a modified simulation platform called Fractional-Order Diffusion Mobile Actuator-Sensor 2-Dimension Fractional-Order Proportional Integral (FO-Diff-MAS2D-FOPI). Finally, extensive numerical simulations for the tempered anomalous diffusion process are presented to verify the effectiveness of our proposed fractional-order PI controllers.

1. Introduction

Tempered anomalous diffusion is a diffusion process with a nonlinear relationship to time, unlike normal diffusion applied in biomedical systems [1,2], in which the mean squared displacement is a linear function of time. In contrast to anomalous diffusion, tempered anomalous diffusion is described by an exponentially tempered power law, whose equations based on tempered fractional derivatives [3] form a useful extension. Specifically, in our work, we study the tempered anomalous diffusion system governed by the time tempered fractional diffusion equation. As we know, tempered time fractional derivatives are generated by tempered power law waiting times, which arise in the Fokker-Planck equation corresponding to the continuous time random walk (CTRW) model with tempered waiting time measure [4,5]. A tempered fractional calculus where power laws were tempered by an exponential factor, was promoted in [6], as a more flexible alternative for practical applications. It is proven that the tempered fractional diffusion model is very useful to finance [7,8] and geophysics [9,10] in some applications. In a tempered anomalous diffusion process, static sensors for pollution measurement are deployed to cover the whole polluted area and gather pollution concentration information while the mobile actuators equip with limited chemical neutralizers for eliminating pollution by properly spraying chemical substances.

Our work on controlling the tempered anomalous diffusion process with a static pollution source is motivated by the application of Centroidal Voronoi Tessellations (CVTs) [11,12], mobile actuator-sensor networks (MASs) [13], and Unmanned Aerial Systems (UASs) [14]. Coverage control was provided by Cortés et al. [12] for multivehicle networks, which can be viewed as a novel approach to coordination algorithm for mobile sensing networks. Notable work on several probabilistic algorithms and their parallel implementations for determining CVTs was presented in [15]. Additionally, monitoring and controlling of the spatially distributed diffusion process based on MASs have been primarily investigated by Chen et al. [13,16] in the past few years. As technology advances beyond our ability to keep track of it, UASs are used for agricultural applications, for example, solving minimal negative impact caused by pest and pesticide to the soil based on the simulation platform named Fractional-Order Diffusion Mobile Actuator-Sensor 2-Dimension (FO-Diff-MAS2D) [17].

Motivated by the argument of why consider fractional-order controllers even when integer-order controller can implement comparatively well for fractional-order systems in [18] and the application of tempered anomalous diffusion systems, in this paper, we try to solve the pollution neutralization spraying control problem for a tempered anomalous diffusion system utilizing the fractional-order PI controllers. The fractional-order proportional

* Corresponding author at: Key Laboratory of Advanced Process Control for Light Industry (Ministry of Education), Jiangnan University, Wuxi 214122, PR China.
E-mail addresses: karenchenjuan.student@sina.com (J. Chen), bozhuang@vip.jiangnan.edu.cn (B. Zhuang), yqchen@ieee.org, ychen53@ucmerced.edu (Y. Chen), btcui@jiangnan.edu.cn (B. Cui).

http://dx.doi.org/10.1016/j.isatra.2017.04.005
0019-0578/

integral derivative (FO-PID) controller proposed in [19], which involves the fractional-order integrator and the fractional-order differentiator. More recently, there has been some considerable contribution on the fractional-order controller [20] and the fractional-order system [21,22]. Oustaloup [20] developed CRONE controller for controlling dynamic systems, which had better performance than the conventional proportional integral derivative (PID) controller when it was used to control fractional-order systems. In the work [23], Özdemir also verified that the fractional-order PI^{λ} controller was more effective than the classical proportional integral (PI) controller for the system subject to input Duhem hysteresis. In [21,22], Chen et al. first investigated the robust stability problem of uncertain fractional-order linear time-invariant systems with interval coefficients and used Lyapunov inequality to test robust stability of the linear time-invariant interval fractional-order system.

Despite the considerable contribution of neutralization control for the anomalous diffusion process and the tempered anomalous diffusion process based on the integer-order controller in [17,24], very few results are available on diffusion control for the tempered anomalous diffusion system utilizing the fractional-order controller. Actually, from engineering point of view, computation maybe faster and memory maybe cheaper, which make the application of fractional calculus, including fractional-order systems and fractional-order controllers, available and reasonable [18,25]. What's more, the fractional-order controller can adjust the dynamical properties of the fractional-order system thanks to the flexible property of the fractional-order controller [19], and fractional-order control is ubiquitous based on real world dynamic systems examples with distributed parameter nature [18]. In the context, we argue that one needs to take into account the integration that encompasses the tempered anomalous diffusion system and the fractional-order PI controller. More specifically, we introduce the fractional-order PI controller for controlling the tempered fractional anomalous diffusion system with a static pollution source and a moving pollution source. Furthermore, based on Diff-MAS2D [26] and FO-Diff-MAS2D [24,17], a modified simulation platform called FO-Diff-MAS2D-FOPI is introduced. We hope that our results here could provide some insights into the diffusion control analysis of the tempered anomalous diffusion systems using the fractional-order PI controller.

Preliminaries and mathematical tools are introduced in Section 2 briefly. Mathematical modeling and problem statement are presented in Section 3. Section 4 is contributed to diffusion control for actuator motion and spraying problems. In Section 5, we present FO-DIFF-MAS2D-FOPI simulation platform and two numerical experiments with static and moving pollution sources based on the proposed fractional-order PI controllers. Finally, conclusions and some future work can be found in Section 6.

2. Preliminaries and mathematical tools

In this section, we first illustrate the definitions and some properties on fractional calculus and tempered fractional calculus, and then introduce the fractional-order PI controller.

2.1. Fractional calculus and tempered fractional calculus

Some definitions about fractional calculus and tempered fractional derivatives are presented. Specifically, we introduce the left Caputo fractional derivative, the left Caupto tempered fractional derivative, and the Riemann-Liouville fractional calculus, respectively.

Suppose $0<\alpha<1$, $\lambda\geq 0$, the left Caputo fractional derivative and the left Caputo tempered fractional derivative with respect to the order of α and the function of $f(t)$ are given by [27,5,28]

$$ {}_0^C D_t^{\alpha} f(t) = \frac{1}{\Gamma(1-\alpha)} \int_0^t (t-s)^{-\alpha} f'(s)\mathrm{d}s, \tag{1}$$

and

$$\begin{aligned} {}_0^C D_t^{\alpha,\lambda} f(t) &= e^{-\lambda t}\, {}_0^C D_t^{\alpha}[e^{\lambda t} f(t)] \\ &= e^{-\lambda t} \frac{1}{\Gamma(1-\alpha)} \int_0^t (t-s)^{-\alpha} [e^{\lambda s} f(s)]'\mathrm{d}s, \end{aligned} \tag{2}$$

where $\Gamma(\cdot)$ represents Gamma function defined by $\Gamma(\alpha)=\int_0^{\infty} e^{-t} t^{\alpha-1}\mathrm{d}t$.

Likewise, the left Riemann-Liouville fractional integral of the β-th order $(0<\beta<1)$ [27,28] can be defined as follows

$$ {}_0 D_t^{-\beta} f(t) = \frac{1}{\Gamma(\beta)} \int_0^t (t-s)^{\beta-1} f(s)\mathrm{d}s. \tag{3}$$

The left Riemann-Liouville fractional derivative is described by

$$ {}_0 D_t^{\beta} f(t) = \frac{1}{\Gamma(1-\beta)} \frac{\mathrm{d}}{\mathrm{d}t} \int_0^t (t-s)^{-\beta} f(s)\mathrm{d}s, \tag{4}$$

where $0<\beta<1$.

According to the above definitions, we can obtain the property of the Riemann-Liouville fractional derivative as follows [27]

$$ \frac{\mathrm{d}}{\mathrm{d}t}\left({}_0 D_t^{-\beta} f(t)\right) = {}_0 D_t^{1-\beta} f(t), \tag{5}$$

where $0<\beta<1$.

Remark 1. According to the above definitions of the left Riemann-Liouville fractional derivative and the left Caputo fractional derivative, we can get the left Caputo fractional derivative of function $f(t)$ with initial value $f(0)=0$ and the β-th order $(0<\beta<1)$ based on [25, Property 3] as below

$$\begin{aligned} {}_0^C D_t^{\beta} f(t) &= \frac{1}{\Gamma(1-\beta)} \int_0^t (t-s)^{-\beta} f'(s)\mathrm{d}s \\ &= {}_0 D_t^{\beta-1} f'(t) = {}_0 D_t^{\beta-1}\left(\frac{\mathrm{d}}{\mathrm{d}t} f(t)\right) \\ &= {}_0 D_t^{\beta} f(t) - \sum_{i=1}^{2} \left[{}_0 D_t^{1-i} f(t)\right]_{t=0} \frac{t^{1-\beta-i}}{\Gamma(2-\beta-i)}. \end{aligned} \tag{6}$$

Since $f(0)=0$, we can obtain

$$ {}_0^C D_t^{\beta} f(t) = {}_0 D_t^{\beta} f(t), \tag{7}$$

which implies that the left Caputo fractional derivative is equal to the left Riemann-Liouville fractional derivative with the same function and the same order when the initial value of function is equal to 0.

2.2. Fractional-order PI controller

In this section, we propose the generalized fractional-order PI controller with the integral order $\beta\in(0,1)$, which can be written as the fractional-order PI^{β} controller. The transfer function of the proposed controller is given as below [19]

$$ G_f(s) = \frac{U(s)}{E(s)} = H_p + H_i s^{-\beta}, \quad \beta > 0, \tag{8}$$

where $G_f(s)$, $U(s)$, and $E(s)$ represent the transfer function of the proposed controller, the output of the proposed controller, and the error, respectively. H_p is the proportional gain, H_i is the integral gain.

Considering the inverse Laplace transform for the above transfer function (8), we obtain the unit-impulse response of the proposed controller as follows

$$U(t) = H_p e(t) + H_{i0} D_t^{-\beta} e(t), \quad \beta > 0. \tag{9}$$

3. Mathematical modeling and problem statement

In this section, we consider the following tempered anomalous diffusion system to illustrate dynamic process of pollution concentration, and then introduce some basic knowledge on CVTs. The motivation for choosing this system is that the partial differential equation can describe the dynamic behavior of the anomalous diffusion process exactly. Moreover, the control force added to this system takes a considerable effect to the tempered anomalous diffusion problem.

3.1. Tempered anomalous diffusion system

In a convex polytope $\Theta \in \mathcal{R}^2$, we assume that a tempered anomalous diffusion process occurs with the time domain $t \geq 0$ and a group of m mobile actuators moves to a certain location freely in this region. Let the set $L = \{l_1, l_2, \ldots, l_m\}$ be the position coordinate set of mobile actuators, where l_i denotes the position coordinate of the i-th mobile robot. $\varphi(x, y, t)$ represents the pollution concentration of the area Θ. The Caputo tempered fractional derivative is used to formulate the dynamic process, which is given by

$${}_0^C D_t^{\alpha,\lambda} \varphi(x, y, t) = k\left(\frac{\partial^2 \varphi}{\partial x^2} + \frac{\partial^2 \varphi}{\partial y^2}\right) + \sum_{i=1}^{m} g(x, y; l_i(t)) u_{s_i}(t) + f_d(x, y, t), \tag{10}$$

where ${}_0^C D_t^{\alpha,\lambda}(\cdot)$ represents the Caputo tempered fractional derivative, $0 < \alpha < 1$, $\lambda > 0$, l_i is the location coordinate of the i-th actuator, $g(\cdot)$ is the shape function, which means the implementation scope of mobile actuators, $u_{s_i}(\cdot)$ represents the control force for the i-th actuator spraying, $f_d(\cdot)$ is the pollution source, k is a positive diffusion coefficient.

The exact formats of $g(x, y; l_i(t))$ and $u_{s_i}(t)$ depend on the specific control performance requirement determined by users. Suppose that each actuator can receive the information from static sensors. Then, by taking advantage of the control law, the mobile robots move to high density of pollution and release the neutralization chemical materials. The corresponding control objectives are as follows

- To control the tempered anomalous diffusion process rationally and reduce pollutants.
- To minimize the polluted area that is heavily affected.
- To neutralize the pollutants as quickly as possible.

3.2. Fundamentals of CVTs

First, according to the actuators position, let us divide Θ into a set of m polytopes $\Pi = \{V_1, \ldots, V_m\}$, where $l_i \in V_i$. Assume that for every $i \in \{1, \ldots, m\}$, then there exists

$$V_i = \{l \in \Theta \,|\, |l - l_i| < |l - l_j| \text{for} j = 1, \ldots, m, j \neq i\}, \tag{11}$$

where $|\cdot|$ represents the Euclidean distance, and l is an arbitrary point in the area Θ. We can obtain $V_i \cap V_j = \varnothing$ for $i \neq j$ and $\cup_{i=1}^m \bar{V}_i = \bar{\Theta}$, where $\bar{V}_i = V_i \cup \partial V_i$, $\bar{\Theta} = \Theta \cup \partial\Theta$.

Then, we define the set of regions $(V_i)_{i=1}^m$ as the Voronoi diagram which is generated by the set of points $(l_i)_{i=1}^m$. If V_i is adjacent to V_j, we take the point l_i as a neighbor of the point l_j. For each Voronoi cell V_i and the density function $\rho(l) \geq 0$ defined on $\bar{\Theta}$, we suppose that the density function $\rho(l)$ satisfies

$$\rho(l) = \varphi(l).$$

Define some basic concepts referred to mass and centroid (center of mass) [12], which are given by

$$M_{V_i} := \int_{V_i} \varphi(l) \mathrm{d}l, \quad \forall\, i \in \{1, \ldots, m\}, \tag{12}$$

and

$$\bar{l}_i := \frac{1}{M_{V_i}} \int_{V_i} l\varphi(l) \mathrm{d}l, \quad \forall\, i \in \{1, \ldots, m\}. \tag{13}$$

It is noticeable that if the generators $(l_i)_{i=1}^m$ are also the centroids of their Voronoi cells, whose mathematical expression can be described by

$$l_i = \bar{l}_i, \quad \forall\, i \in \{1, \ldots, m\}, \tag{14}$$

such Voronoi tessellations are called CVTs.

Next, we present an example on CVTs, which can be constructed by 20 random points in the area Θ with density function $\varphi(x, y) = e^{-8(x-0.3)^2 - 8(y-0.3)^2}$, as shown in Fig. 1(a). Generally speaking, in reality, Voronoi configurations are generated by the trajectories of mobile actuators at a certain time rather than the actuators location, which is shown in Fig. 1(b).

4. Diffusion control for the tempered anomalous diffusion system

As we know, diffusion control for a tempered anomalous diffusion problem can be separated into two subproblems:

(1) Actuator motion control problem (where to go for mobile actuators).
(2) Actuator spraying control problem (how much to spray for mobile actuators).

In what follows, the discussion on them will be presented in some detail.

4.1. Actuator motion problem formulation

In order to control the tempered anomalous diffusion problem and reduce the amount of pollutants, it is obvious that if the mobile actuators get closer to the high-concentration polluted area and are further from lightly polluted area, control effect will be better. However, since the diffused pollutants far away from the source also need to be eliminated timely, it is unreasonable to put all the mobile actuators close to the pollution source. As is illustrated in above analysis, we introduce the below cost function, which needs to be minimized in [12,16].

$$\mathcal{H}(L, \Pi) = \sum_{i=1}^{m} \int_{V_i} \varphi(l) |l - l_i|^2 \, \mathrm{d}l \quad \text{for} l \in \Theta,$$
$$\text{s. t.} \quad |\dot{l}_i| < h_{vel}, |\ddot{l}_i| < h_{acc}, \quad \forall\, i \in \{1, \ldots, m\}, \tag{15}$$

where $\varphi(l)$ represents concentration at the point l in the area Θ, h_{vel} and h_{acc} denote the upper bounds of the velocity and the acceleration of mobile actuators, respectively.

To simplify the expression, we write

$$\mathcal{H}_L = \mathcal{H}(L, \Pi).$$

Furthermore, as the Voronoi diagrams $(V_i)_{i=1}^m$ depend at least

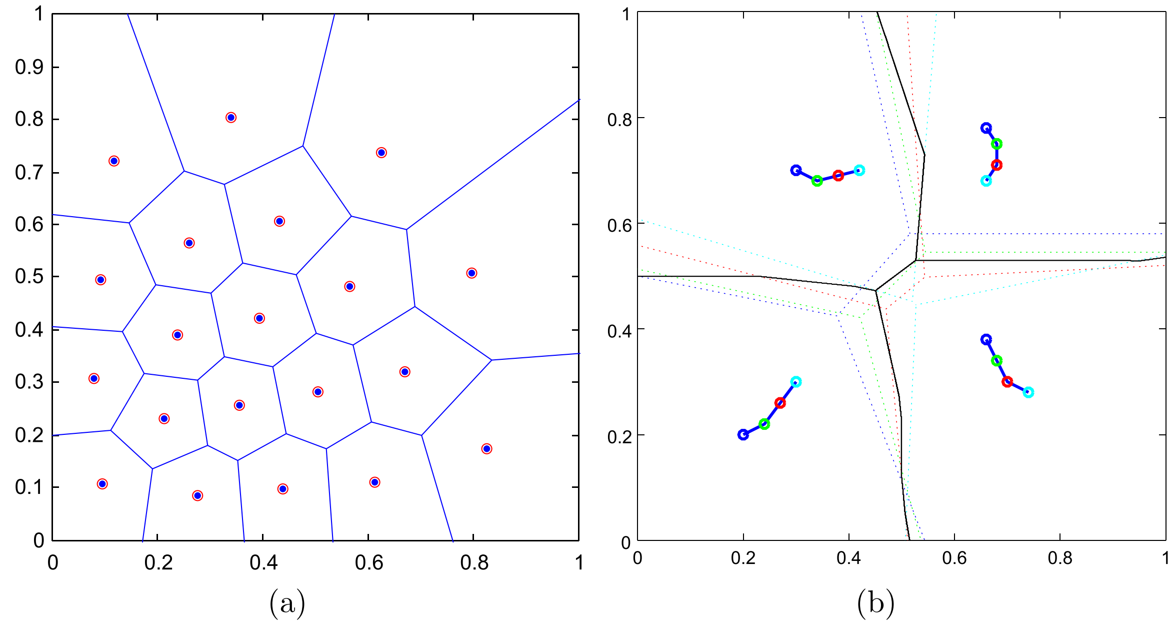

Fig. 1. CVTs constructed by 20 random points and trajectories of 4 mobile actuators.

continuously on the set $L = (l_1, \ldots, l_m)$ for all $l_i \neq l_j$, we can deduce that the function $\mathcal{H}_L$ is at least continuously differentiable with respect to time t.

By taking advantage of the parallel axis theorem and some basic definitions of CVTs given in (12) and (13), the partial derivative of the cost function $\mathcal{H}_L$ can be obtained as below

$$\frac{\partial \mathcal{H}_L}{\partial l_i} = 2M_{V_i}\left(l_i - \bar{l}_i\right), \quad \forall\, i \in \{1, \ldots, m\}. \tag{16}$$

Following [16,15], that $\{l_i, V_i\}_{i=1}^{m}$ is a CVT of Θ can be a necessary condition to minimize $\mathcal{H}_L$. For the above function $\mathcal{H}_L$, the local minimum points are centroids of their Voronoi cells, which implies that each actuator position is the generator for current Voronoi configuration and its centre of mass. We can describe it as follows

$$\bar{l}_i = \underset{l_i}{\operatorname{argmin}} \mathcal{H}_L, \quad \forall\, i \in \{1, \ldots, m\}.$$

To compute the desired location of mobile actuators, we use Lloyd's method as a deterministic algorithm to generate Centroid Voronoi cells [16]. Although Lloyd's method converges faster than probabilistic methods due to fewer iterations, computation requirements are higher for this method, which can be addressed by a modificatory distribution algorithm [12,16] with the advantage in reducing the computation amount.

4.2. Fractional-order PI controller for actuator motion planning

In this paper, suppose the mobile actuators are treated as virtual particles. In what follows, each i comes from the set $\{1, \ldots, m\}$. The mobile actuators location follows the second-order dynamical equation below

$$\ddot{l}_i = u_{l_i}. \tag{17}$$

We describe the right part of the above equation clearly as follows

$$u_{l_i} = f_i - h_v \dot{l}_i, \tag{18}$$

where f_i is the force input to control the motion of the robot by CVT and is given by a fractional-order PI controller

$$f_i = h_p\left(\bar{l}_i - l_i\right) + h_i\, {}_0D_t^{-\beta}\left(\bar{l}_i - l_i\right). \tag{19}$$

Substituting (19) into (18), we can obtain

$$u_{l_i} = h_p\left(\bar{l}_i - l_i\right) + h_i\, {}_0D_t^{-\beta}\left(\bar{l}_i - l_i\right) - h_v \dot{l}_i, \tag{20}$$

where h_p and h_i are a positive proportional coefficient, and a positive integral coefficient, respectively. Generally, they are determined by designer based on practical requirements of engineering.

According to (17), the above equation can be rewritten

$$\ddot{l}_i = h_p\left(\bar{l}_i - l_i\right) + h_{i0} D_t^{-\beta}\left(\bar{l}_i - l_i\right) - h_v \dot{l}_i. \tag{21}$$

Note that, according to the equation (5), it is easy to obtain

$$\frac{\mathrm{d}}{\mathrm{d}t}\left({}_0D_t^{-\beta}\left(l_i - \bar{l}_i\right)\right) = {}_0D_t^{1-\beta}\left(l_i - \bar{l}_i\right). \tag{22}$$

Remark 2. The second term of (18) on the right hand side is the viscous friction artificially given in [29], in which h_v is a positive constant and $\dot{l}_i$ represents the velocity of the i-th mobile robot. Moreover, h_v equals the proportion of viscosity coefficient to agent mass. In particular, h_v=1 means the viscosity coefficient equals to agent mass. The viscous term is used to eliminate the oscillation behavior of mobile robots when the robots are very close to the destination, which guarantees that the robot will come to a standstill eventually in the absence of the external force.

4.3. Convergence to centroidal Voronoi tessellations under the fractional-order PI controller

Next, we study the fractional-order PI control design for nonlinear passive-dynamics system [30], which can be regarded as the extension of integer-order control design [12]. In Section 4.2, we considered the dynamic system described by a second-order motion equation (17) for each actuator. In particular, we supposed that the above controlled system's dynamics is passive with input u_{l_i} and output $\dot{l}_i$ in (20), which can infer that the input u_{l_i} is equal to 0 with the zero-dynamics manifold $\dot{l}_i = 0$. In this paper, we choose the general form of the fractional-order PI controller for control input

$$u_{l_i} = -h_{pro}M_{V_i}\left(l_i - \bar{l}_i\right) - h_{int}M_{V_i 0}D_t^{-\beta}\left(l_i - \bar{l}_i\right) - h_v\dot{l}_i, \tag{23}$$

where $h_{pro} > 0$, $h_{int} > 0$, $h_v > 0$ are henceforth called scale positive gains.

Based on (17) and (23), we can re-write the second-order dynamical equation of each actuator as follows

$$\ddot{l}_i = u_{l_i} = -h_{pro}M_{V_i}\left(l_i - \bar{l}_i\right) - h_{int}M_{V_i 0}D_t^{-\beta}\left(l_i - \bar{l}_i\right) - h_v\dot{l}_i. \tag{24}$$

It is known that the CVT can solve the time-invariant environment problem with the time-independence state function. However, when the evolution rate of the tempered anomalous diffusion process is agonisingly slow comparing with the convergence rate of the Lloyd's method, the CVT can still keep the validation for our problem. Moreover, as the Lloyd's method is executed periodically, the motion of mobile actuators can be adaptive to the evolution of the tempered anomalous diffusion process. Therefore, in this paper, the actuators location can still converge to a CVT based on the control input (23) with a fractional-order PI controller in the time-varying environment, which is verified through the simulation results in Section 5.2.

In the following theorem, we design a control input with some certain conditions, in spirit of results proposed in [12], which can guarantee that the mobile actuators position converges to the centroid of Voronoi configuration. The main difference between the work given in [12] and ours is that we investigate the dynamical behavior of each actuator described by the control input with a fractional-order PI controller and a certain condition on its scale gains, instead of the dynamical system represented by a control input with the integer-order P controller for each sensor.

Theorem 1. *For the above second-order dynamical behavior (17) induced by a control input (23) for each actuator, if the control input is derived by the fractional-order PI controller and its scale gains satisfy $h_{pro} > h_{int} > 0$ and $h_v=1$, then the above second-order dynamic system of each actuator (24) is asymptotically stable via the proposed control input (23), which implies that the actuators location asymptotically converges to the centroid of Voronoi cell.*

proof. Consider the following Lyapunov function

$$\Upsilon(t) = \frac{1}{2}(h_{pro} - h_{int}h_v)\mathcal{H}_L + \frac{1}{2}\sum_{i=1}^{m}\left(\sqrt{h_{int}h_vM_{V_i}}(l_i - \bar{l}_i) + \sqrt{h_{int}h_vM_{V_i 0}}D_t^{-\beta}(l_i - \bar{l}_i)\right)^2 + \frac{1}{2}\sum_{i=1}^{m}\left(\dot{l}_i + h_v(l_i - \bar{l}_i)\right)^2. \tag{25}$$

Obviously, the proposed Lyapunov function $\Upsilon(t) > 0$ for $h_{pro} > h_{int} > 0$ and $h_v=1$. The derivative of the proposed Lyapunov function is given by

$$\begin{aligned}\frac{d\Upsilon(t)}{dt} = {} & \frac{1}{2}\sum_{i=1}^{m}(h_{pro} - h_{int}h_v)\frac{\partial\mathcal{H}_L}{\partial l_i}\dot{l}_i + \sum_{i=1}^{m}\left(\sqrt{h_{int}h_vM_{V_i}}(l_i - \bar{l}_i) + \sqrt{h_{int}h_vM_{V_i 0}}D_t^{-\beta}(l_i - \bar{l}_i)\right)\\ & \times\left(\sqrt{h_{int}h_vM_{V_i}}\dot{l}_i + \sqrt{h_{int}h_vM_{V_i}}\frac{d}{dt}\left({}_0D_t^{-\beta}(l_i - \bar{l}_i)\right)\right)\\ & + \sum_{i=1}^{m}\left(\dot{l}_i + h_v(l_i - \bar{l}_i)\right)(\ddot{l}_i + h_v\dot{l}_i).\end{aligned}$$

Using the formulation of $\frac{\partial\mathcal{H}_L}{\partial l_i}$, $\ddot{l}_i$ and $\frac{d}{dt}\left({}_0D_t^{-\beta}\left(l_i - \bar{l}_i\right)\right)$ given by (16), (24) and (22), we have

$$\begin{aligned}\frac{d\Upsilon(t)}{dt} = {} & \sum_{i=1}^{m}(h_{pro} - h_{int}h_v)M_{v_i}\dot{l}_i(l_i - \bar{l}_i)\\ & + \sum_{i=1}^{m}h_{int}h_vM_{v_i}\dot{l}_i(l_i - \bar{l}_i)\\ & + \sum_{i=1}^{m}h_{int}h_vM_{v_i}(l_i - \bar{l}_i)_0D_t^{1-\beta}(l_i - \bar{l}_i)\\ & + \sum_{i=1}^{m}h_{int}h_vM_{v_i}\dot{l}_{i0}D_t^{-\beta}(l_i - \bar{l}_i)\\ & + \sum_{i=1}^{m}h_{int}h_vM_{v_i 0}D_t^{-\beta}(l_i - \bar{l}_i)_0D_t^{1-\beta}(l_i - \bar{l}_i)\\ & - \sum_{i=1}^{m}h_{pro}M_{v_i}\dot{l}_i(l_i - \bar{l}_i)\\ & - \sum_{i=1}^{m}h_{int}M_{v_i}\dot{l}_{i0}D_t^{-\beta}(l_i - \bar{l}_i)\\ & - \sum_{i=1}^{m}h_vh_{pro}M_{v_i}(l_i - \bar{l}_i)^2\\ & - \sum_{i=1}^{m}h_vh_{int}M_{v_i}(l_i - \bar{l}_i)_0D_t^{-\beta}(l_i - \bar{l}_i).\end{aligned}$$

Moreover, since $h_{pro} > 0$, $h_{int} > 0$, $h_v = 1$, we infer that

$$\begin{aligned}\frac{d\Upsilon(t)}{dt} = {} & \sum_{i=1}^{m}h_{int}M_{v_i}\left(l_i - \bar{l}_i\right)_0D_t^{1-\beta}\left(l_i - \bar{l}_i\right)\\ & + \sum_{i=1}^{m}h_{int}M_{v_i 0}D_t^{-\beta}\left(l_i - \bar{l}_i\right)_0D_t^{1-\beta}\left(l_i - \bar{l}_i\right)\\ & - \sum_{i=1}^{m}h_{pro}M_{v_i}\left(l_i - \bar{l}_i\right)^2\\ & - \sum_{i=1}^{m}h_{int}M_{v_i}\left(l_i - \bar{l}_i\right)_0D_t^{-\beta}\left(l_i - \bar{l}_i\right).\end{aligned}$$

In order to simplify the proof, we set

$$\frac{d\Upsilon(t)}{dt} = \dot{\Upsilon}_1(t) + \dot{\Upsilon}_2(t) + \dot{\Upsilon}_3(t) + \dot{\Upsilon}_4(t),$$

where

$$\begin{aligned}\dot{\Upsilon}_1(t) &= \sum_{i=1}^{m}h_{int}M_{v_i}\left(l_i - \bar{l}_i\right)_0D_t^{1-\beta}\left(l_i - \bar{l}_i\right),\\ \dot{\Upsilon}_2(t) &= \sum_{i=1}^{m}h_{int}M_{v_i 0}D_t^{-\beta}\left(l_i - \bar{l}_i\right)_0D_t^{1-\beta}\left(l_i - \bar{l}_i\right),\\ \dot{\Upsilon}_3(t) &= -\sum_{i=1}^{m}h_{pro}M_{v_i}\left(l_i - \bar{l}_i\right)^2,\\ \dot{\Upsilon}_4(t) &= -\sum_{i=1}^{m}h_{int}M_{v_i}\left(l_i - \bar{l}_i\right)_0D_t^{-\beta}\left(l_i - \bar{l}_i\right).\end{aligned}$$

Next, let us investigate each function of $\dot{\Upsilon}_k(t)$ $(k = 1, 2, 3, 4)$ is positive or negative as follows

(1) Suppose $\dot{\Upsilon}_{1i}(t) = h_{int}M_{v_i}\left(l_i - \bar{l}_i\right)_0D_t^{1-\beta}\left(l_i - \bar{l}_i\right)$, then

$$\dot{\Upsilon}_1(t) = \sum_{i=1}^{m}\dot{\Upsilon}_{1i}(t).$$

To prove $\dot{\Upsilon}_1(t) \le 0$, it is equivalent to prove that

$$\left(l_i - \bar{l}_i\right)_0D_t^{1-\beta}\left(l_i - \bar{l}_i\right) \le 0.$$

According to the definition of the Riemann-Liouville fractional derivative, we have

Please cite this article as: Juan Chen, et al. Diffusion control for a tempered anomalous diffusion system using fractional-order PI controllers. ISA Transactions (2017), http://dx.doi.org/10.1016/j.isatra.2017.04.005

$$\left(l_i-\bar{l}_i\right){}_0D_t^{1-\beta}\left(l_i-\bar{l}_i\right)=\frac{l_i-\bar{l}_i}{\Gamma(\beta)}\frac{\mathrm{d}}{\mathrm{d}t}\int_0^t(t-s)^{\beta-1}\left(l_i-\bar{l}_i\right)\mathrm{d}s.$$

Consider the property of CVT algorithm on the convergence rate of the Lloyd's method, suppose the actuators position l_i converges to its CVT centroids faster than $t^{\beta-1}$ [31], then we can discuss the plus or minus of $\left(l_i-\bar{l}_i\right){}_0D_t^{1-\beta}\left(l_i-\bar{l}_i\right)$ in two following cases.

- In the first case, let us take $\left(l_i-\bar{l}_i\right)>0$, and the integral $\int_0^t(t-s)^{\beta-1}\left(l_i-\bar{l}_i\right)\mathrm{d}s$ is monotonically decreasing. Hence,
$$\frac{\mathrm{d}}{\mathrm{d}t}\int_0^t(t-s)^{\beta-1}\left(l_i-\bar{l}_i\right)\mathrm{d}s\le 0,$$
it is noticeable that $\left(l_i-\bar{l}_i\right){}_0D_t^{1-\beta}\left(l_i-\bar{l}_i\right)\le 0$.
- In the second case, let us take $\left(l_i-\bar{l}_i\right)<0$, and the integral $\int_0^t(t-s)^{\beta-1}\left(l_i-\bar{l}_i\right)\mathrm{d}s$ is monotonically increasing, so that the derivative of the above integral is greater than or equal to 0. Obviously, we have
$$\left(l_i-\bar{l}_i\right){}_0D_t^{1-\beta}\left(l_i-\bar{l}_i\right)\le 0.$$

Given the above analysis, we can easily obtain $\left(l_i-\bar{l}_i\right){}_0D_t^{1-\beta}\left(l_i-\bar{l}_i\right)\le 0$, for each case.

(2) Suppose $\dot{\Upsilon}_{2i}(t)=h_{int}M_{V_i}{}_0D_t^{-\beta}\left(l_i-\bar{l}_i\right){}_0D_t^{1-\beta}\left(l_i-\bar{l}_i\right)$, then

$$\dot{\Upsilon}_2(t)=\sum_{i=1}^m\dot{\Upsilon}_{2i}(t).$$

In order to prove $\dot{\Upsilon}_2(t)\le 0$, we have to prove that

$${}_0D_t^{-\beta}\left(l_i-\bar{l}_i\right){}_0D_t^{1-\beta}\left(l_i-\bar{l}_i\right)\le 0.$$

Consider the Riemann-Liouville fractional derivative definition given above, we can obtain

$$\begin{aligned}{}_0D_t^{-\beta}\left(l_i-\bar{l}_i\right)&=\frac{1}{\Gamma(\beta)}\int_0^t(t-s)^{\beta-1}\left(l_i-\bar{l}_i\right)\mathrm{d}s\\&=\frac{1}{\Gamma(\beta+1)}\frac{\mathrm{d}}{\mathrm{d}t}\int_0^t(t-s)^{\beta}\left(l_i-\bar{l}_i\right)\mathrm{d}s,\end{aligned}$$

and

$${}_0D_t^{1-\beta}\left(l_i-\bar{l}_i\right)=\frac{1}{\Gamma(\beta)}\frac{\mathrm{d}}{\mathrm{d}t}\int_0^t(t-s)^{\beta-1}\left(l_i-\bar{l}_i\right)\mathrm{d}s.$$

Thus, it is time to discuss the sign of ${}_0D_t^{-\beta}\left(l_i-\bar{l}_i\right){}_0D_t^{1-\beta}\left(l_i-\bar{l}_i\right)$ in the below cases.

- In the first case, we assume $\left(l_i-\bar{l}_i\right)>0$, then the integral $\int_0^t(t-s)^{\beta}\left(l_i-\bar{l}_i\right)\mathrm{d}s$ is monotonically increasing. Moreover, suppose $\left(l_i-\bar{l}_i\right)>0$ and $\int_0^t(t-s)^{\beta-1}\left(l_i-\bar{l}_i\right)\mathrm{d}s$ is monotonically decreasing. So that,
$$\frac{\mathrm{d}}{\mathrm{d}t}\int_0^t(t-s)^{\beta}\left(l_i-\bar{l}_i\right)\mathrm{d}s\ge 0,$$
$$\frac{\mathrm{d}}{\mathrm{d}t}\int_0^t(t-s)^{\beta-1}\left(l_i-\bar{l}_i\right)\mathrm{d}s\le 0,$$
respectively. It is easy to obtain ${}_0D_t^{-\beta}\left(l_i-\bar{l}_i\right){}_0D_t^{1-\beta}\left(l_i-\bar{l}_i\right)\le 0$.
- In the second case, we take $\left(l_i-\bar{l}_i\right)<0$. Hence, the integral $\int_0^t(t-s)^{\beta}\left(l_i-\bar{l}_i\right)\mathrm{d}s$ is monotonically decreasing, therefore the derivative of this integral is less than or equal to 0. In addition, since the integral $\int_0^t(t-s)^{\beta-1}\left(l_i-\bar{l}_i\right)\mathrm{d}s$ is monotonically increasing, then the corresponding derivative is greater than or equal to 0. As a result, we also have
$${}_0D_t^{-\beta}\left(l_i-\bar{l}_i\right){}_0D_t^{1-\beta}\left(l_i-\bar{l}_i\right)\le 0.$$

By the above analysis, we get that

$${}_0D_t^{-\beta}\left(l_i-\bar{l}_i\right){}_0D_t^{1-\beta}\left(l_i-\bar{l}_i\right)\le 0.$$

(3) Suppose $\dot{\Upsilon}_{3i}(t)=-h_{pro}M_{v_i}\left(l_i-\bar{l}_i\right)^2$, then

$$\dot{\Upsilon}_3(t)=\sum_{i=1}^m\dot{\Upsilon}_{3i}(t).$$

Using the above assumption, we obtain $\dot{\Upsilon}_3(t)\le 0$.

(4) Suppose $\dot{\Upsilon}_{4i}(t)=-h_{int}M_{v_i}\left(l_i-\bar{l}_i\right){}_0D_t^{-\beta}\left(l_i-\bar{l}_i\right)$, then

$$\dot{\Upsilon}_4(t)=\sum_{i=1}^m\dot{\Upsilon}_{4i}(t).$$

For the purpose of proving $\dot{\Upsilon}_4(t)\le 0$, it needs to prove that

$$\left(l_i-\bar{l}_i\right){}_0D_t^{-\beta}\left(l_i-\bar{l}_i\right)\ge 0.$$

Given the definition of Riemann-Liouville derivative, we get

$$\begin{aligned}\left(l_i-\bar{l}_i\right){}_0D_t^{-\beta}\left(l_i-\bar{l}_i\right)&=\frac{l_i-\bar{l}_i}{\Gamma(\beta)}\int_0^t(t-s)^{\beta-1}\left(l_i-\bar{l}_i\right)\mathrm{d}s\\&=\frac{l_i-\bar{l}_i}{\Gamma(\beta+1)}\frac{\mathrm{d}}{\mathrm{d}t}\int_0^t(t-s)^{\beta}\left(l_i-\bar{l}_i\right)\mathrm{d}s.\end{aligned}$$

Then, we have to discuss the plus or minus of $\left(l_i-\bar{l}_i\right){}_0D_t^{-\beta}\left(l_i-\bar{l}_i\right)$ in two below cases.

- In the first case, we set $\left(l_i-\bar{l}_i\right)>0$, then the integral $\int_0^t(t-s)^{\beta}\left(l_i-\bar{l}_i\right)\mathrm{d}s$ is monotonically increasing. Therefore,
$$\frac{\mathrm{d}}{\mathrm{d}t}\int_0^t(t-s)^{\beta}\left(l_i-\bar{l}_i\right)\mathrm{d}s\ge 0,$$
it implies that $\left(l_i-\bar{l}_i\right){}_0D_t^{-\beta}\left(l_i-\bar{l}_i\right)\ge 0$.
- In the second case, we set $\left(l_i-\bar{l}_i\right)<0$, then the integral $\int_0^t(t-s)^{\beta}\left(l_i-\bar{l}_i\right)\mathrm{d}s$ is monotonically decreasing. It denotes that the derivative of the above integral is less than or equal to 0. Hence, we have
$$\left(l_i-\bar{l}_i\right){}_0D_t^{-\beta}\left(l_i-\bar{l}_i\right)\ge 0.$$

By the above analysis, we can easily obtain $\left(l_i-\bar{l}_i\right){}_0D_t^{-\beta}\left(l_i-\bar{l}_i\right)\ge 0$ which infers $\dot{\Upsilon}_4(t)\le 0$.

Now, we conclude that $\frac{\mathrm{d}\Upsilon(t)}{\mathrm{d}t}\le 0$, it suffices to apply the above assumption and combine with the above analysis, since $\dot{\Upsilon}_1(t)\le 0$, $\dot{\Upsilon}_2(t)\le 0$, $\dot{\Upsilon}_3(t)\le 0$, $\dot{\Upsilon}_4(t)\le 0$.

Finally, the actuators location can asymptotically converge to the largest invariant set contained in $\dot{l}_i=0$ by LaSalle's invariance principle. According to zero dynamics on above passive-dynamics system, we easily find that $l_i-\bar{l}_i=0$ for $i=1,\ldots,m$, i.e., LaSalle's invariance principle can guarantee convergence to a CVT when the set of centroidal Voronoi configurations is finite. In other words, it infers that the control input (23) with a fractional-order PI control law can stabilize the passive-dynamics system (24) to one of its minima. □

Remark 3. Note that, the proposed theorem also can guarantee the stability of the second-order dynamic system of each actuator

(24). Moreover, the study of the tempered anomalous diffusion system based on the control input with a fractional-order PI control law (19) can be taken as the extension of the normal diffusion system under a control input with the integer-order control law.

4.4. Actuator spraying control problem statement

According to the control objective of the tempered anomalous diffusion problem, pollution should be neutralized as quickly as possible. However, in reality, due to the tempered stable process with long-time heavy tail of the tempered anomalous diffusion system, the total amount of pollution released by the pollution source will decrease itself even if there is no control input. Therefore, to reduce the pollution amount timely, we design a fractional-order PI controller for spraying control rationally, whose validity can be verified by some numerical simulations in Section 5.2 and Section 5.3.

4.5. Fractional-order PI controller for spraying control

Motivated by [32, Chapter 7.3.3] and [19, Sec VI] , in this part of this paper, we turn to use the fractional-order PI controller for neutralizing chemical releasing in the tempered fractional diffusion process. The fractional-order PI controller is a generalization of the integer-order PI controller, which is alternative to the integer-order PI controller. In many cases it can be assumed that the relationship of the amount of chemicals each robot released and the average pollutant concentration in the Voronoi cell belonging to that robot can be denoted by

$$u_{s_i}(t) = -h_{pr}\bar{\varphi}_i(x, y, t) - h_{ir\,0}D_t^{-\gamma}\bar{\varphi}_i(x, y, \tau), \; i = 1, \dots, m, \tag{26}$$

where $\bar{\varphi}_i(x, y, t) = \frac{\int_{\tilde{V}_i}\varphi(x, y, t)\mathrm{d}V}{\int_{\tilde{V}_i}\mathrm{d}V}$ represents the average pollutant concentration, ${}_0D_t^{-\gamma}(\cdot)$ is the left Riemann-Liouville fractional integral with the integral order of γ, h_{pr}, and h_{ir} are positive constants. The above spraying controller gains usually depend on the practical requirements of engineering.

Take $\tilde{V}_i$ as follows

$$\tilde{V}_i = V_i \cap C_i,$$

where $C_i = \{ l \,|\, |l - l_i| < r_i \}$, $i=1,\dots,m$, r_i represents the sensing range of the i-th actuator, and V_i is the Voronoi cell of the i-th actuator.

4.6. FOPI-based CVT algorithm

In this paper, the FOPI-based CVT algorithm contains two critical parts of actuator moving control and actuator neutralization control. We present the new FOPI-based CVT algorithm steps with a proper pseudo code representation as follows

Algorithm 1. FOPI-based CVT algorithm.

- Step 1: Initial settings: actuator position $l_i \in \{l_1, \dots, l_m\}$, disturbance f_d, response time $t = 0$.
- Step 2: Compute Voronoi cells V_i, $i = 1, \dots, m$ generated by actuators.
- Step 3: Get the sensor data within Voronoi cell V_i and compute the mass centroid $\bar{l}_i$ and the average pollution concentration $\bar{\varphi}_i$ in range r_i.
- Step 4: Moving and spraying control: according to (20), compute motion control input u_{l_i}, then in terms of (26) compute the spray control input u_{s_i}.
- Step 5: Repeat step 2 - step 4 until no pollution is detected, then stop.

Remark 4. The FOPI-based CVT algorithm is a non-model algorithm, i.e., it does not need to know the exact mathematical form of the model. Due to the uncertainty of our dynamic model, the proposed control strategy may be uncommon and may have some limitations for the uncertain dynamic system.

5. Simulation results

In this section, we will illustrate the FO-DIFF-MAS2D-FOPI simulation platform and two numerical experiments via the proposed fractional-order PI controllers.

5.1. FO-DIFF-MAS2D-FOPI simulation platform

We consider the area given in uniformization by $\Theta = \{(x, y) | 0 \le x \le 1, 0 \le y \le 1\}$. $M \times N$ sensors distribute in Θ evenly, which forms a network over the area. Meanwhile, it contains m mobile robots, which are in charge of spraying control through releasing the neutralization chemical materials.

Given the property of FO-Diff-MAS-2D simulation platform [24,17], we introduce the fractional-order PI controllers into it for diffusion control of the tempered anomalous diffusion system, which forms the new simulation platform called FO-Diff-MAS2D-FOPI. The time fractional derivative can be discretized by FO-Diff-MAS2D-FOPI, which leaves the time domain integration to Matlab/Simulink. Some main features of FO-Diff-MAS2D-FOPI simulation platform are given as follows

- Sensors and actuators can be collocated or non-collocated.
- Pollution source can be static or moving.
- The mobile actuators can obey first-order or second-order dynamical equation while movement of actuators can be open-loop or closed loop, which is designed by users according to a certain requirement.
- The control force for actuators motion control and spraying control can be an integer-order controller or a fractional-order PI controller, whose algorithm can be an arbitrary control algorithm.

FO-Diff-MAS2D-FOPI simulation platform use the finite difference method (FDM), which is based on discretizing the solution space into grid cells and approximating space fractional derivative over each cell. With the help of [33, page 225] and the Oustaloup algorithm, the fractional-order derivative of the tempered anomalous diffusion system and the fractional-order integral of the proposed fractional-order PI controller are both realized. At every time step, according to the principle of division of the distance closest point, the CVT algorithm is achieved. As usual, we divide the area Θ into 30×30 subdivisions, i.e., 29×29 sensors evenly distributed in Θ.

Dirichlet and Neumann boundary conditions are both available in this simulation platform. In this paper, we choose Neumann boundary condition in the following numerical simulation experiments, which can be described as

$$\frac{\partial\varphi}{\partial\bar{n}} = P_1 + P_2\varphi,$$

where P_1 and P_2 stand for two real constants, $\bar{n}$ is the outward direction to the boundary.

FO-Diff-MAS2D-FOPI simulation platform for actuator motion planing control and actuator spraying control is used to realize two different scenarios given below

(a) A tempered anomalous diffusion process with a static pollution source.
(b) A tempered anomalous diffusion process with a moving pollution source.

where scenario (a) can represent the bacterium in soil that may be viewed as a static source and may have some negative effects on soil, and scenario (b) could be taken as the pest in farmland which may be a moving source and may exert a great negative influence on agricultural production in realistic issues.

On the other hand, we use the fractional-order PI control force to realize the goal of making affected area as small as possible and reducing the total pollution amount as soon as possible. The control performance of the fractional-order PI control force for the tempered anomalous diffusion process can be demonstrated by comparing the following two aspects:

- Variation in the amount of total pollution based on the fractional-order PI controller and without control.
- Evolution of state L_2 norm under the fractional-order PI control force and without control.

In what follows, the simulations for the two scenarios mentioned above use the same set of parameters, i.e., $M=N=29$ meant 30×30 subdivisions in the area Θ, and $m=4$. Fractional-order PI controller is abbreviated as FO-PI controller in following simulation figures.

5.2. Case of static pollution source

We discuss a case of static pollution source first. Suppose four robots work in the case of static pollution source, actuators carrying neutralization chemicals achieve the elimination of pollutants released by the static pollution source of a tempered anomalous diffusion process. The tempered anomalous diffusion process is given by the PDE (10) with control input, where the diffusion coefficient k=0.01, the pollution source $f_d(\cdot)=f_{sd}(\cdot)$ is a static pollution source, $\sum_{i=1}^{m} g(\cdot)u_{s_i}(\cdot)$ is control input for actuator motion planning and spraying control of the static issue. Neumann boundary condition is described as

$$\frac{\partial\varphi}{\partial\bar{n}}=0.$$

We set the static disturbance source as a point disturbance $f_{sd}(\cdot)$ for the tempered anomalous diffusion process. The disturbance equation is $f_{sd}(t)=20e^{-t}\big|_{(x=0.8,y=0.2)}$ with position at (0.8, 0.2). The tempered anomalous process evolves at t=0 to the area Θ with 4 mobile actuators layout on initial positions at (0.33, 0.33), (0.33, 0.66), (0.66, 0.33), (0.66, 0.66), respectively.

To show how mobile actuators make an effort in controlling the diffusion of pollutants, control input is added to the tempered anomalous diffusion process at $t=1.0\,s$. We set the time step $\Delta t=0.004\,s$ so that the mobile actuators recompute their desired position every 0.2 s. The total simulation time is $T=6\,s$.

Based on the previous research work [17,24], we choose the time derivative order $\alpha=0.7$ and tempering parameter $\lambda=1$ in (10) for our numerical simulations. Moreover, to control actuator motion path, we set the viscous coefficient h_v=1, the proportional coefficient h_p=6 and the integral coefficient h_i=1. In order to obtain the optimal fractional order β in (20), we let β vary between 0.4 and 0.9, as shown in Fig. 2. It is worthwhile to note that the second-order dynamic system of each actuator (21) is divergent for $\beta\in(0, 0.4)$ (see Remark 5 for more details).

For the purpose of making pollution amount be lower, we find the optimal fractional order β is 0.9 in the actuator motion control input (20) from the above simulation results in Fig. 2. Then, the actuator motion control input is given by the fractional equation

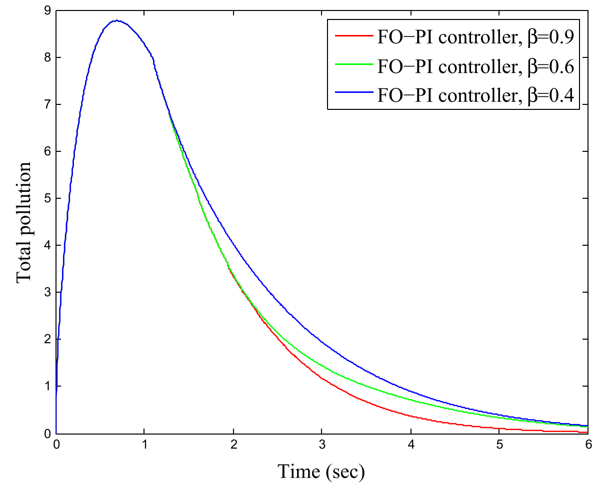

Fig. 2. Evolution of total pollution amount according to different value of β for actuator motion control of a static pollution source.

$$u_{l_i}=6\left(\bar{l}_i-l_i\right)+{}_0D_t^{-0.9}\left(\bar{l}_i-l_i\right)-\dot{l}_i, \tag{27}$$

which also can guarantee the mobile actuators location converges to the centroid of Voronoi configuration along with the mobile actuators' motion, as shown in Fig. 3.

For spraying control, the proportional coefficient is fixed by $h_{pr}=10$. To reduce the total pollution amount as soon as possible, we set h_{ir} to change from 0 to 35 with the step 5 and 10. Under the proposed condition, the evolution of the pollution amount can be seen in Fig. 4, which shows that the bigger h_{ir} is, the better for spraying control. In addition, the evolution of pollution amount is not distinct when $h_{ir}\ge15$, but the total pollutant amount still gets lower as h_{ir} is growing in Fig. 4(b). Therefore, without loss of generality, we take $h_{ir}=15$ in our simulations. Next, in order to obtain the optimal fractional order γ in equation (26), we let γ change from 0.4 to 1.0, the tempered anomalous diffusion system (10) with a static source is also divergent when the corresponding fractional order $\gamma<0.4$ (see Remark 5 for more details). Fig. 5 shows the optimal fractional order γ is 0.7, which can decrease the pollution amount as soon as possible, then we can obtain the spraying control input described by the fractional-order PI controller as follows

$$u_{s_i}(t)=-10\bar{\varphi}_i(x,y,t)-15{}_0D_t^{-0.7}\bar{\varphi}_i(x,y,\tau). \tag{28}$$

To validate the effectiveness of our proposed fractional-order PI control strategy for pollution neutralization, we compare variation of pollutants and evolution of state L_2 norm under the fractional-order PI controllers and without control input in Fig. 6, which shows pollution amount and state L_2 norm with the fractional-order PI control method descend faster than the counterpart without control force. From Table 1, we can find that the amount of total pollution reduces to zero and the state L_2 norm declines to zero after $t=5\,s$ with the fractional-order PI controllers when the counterpart drops to about 0.2 and approximates zero without control at the end of the simulation. As a result, the proposed fractional-order PI control strategy has good control effects for the tempered anomalous diffusion process.

Remark 5. In the case of static pollution source of this paper, based on the Lyapunov stability theory, the actuator's second-order dynamic system (21) must be stable for arbitrary fractional order β. However, if the fractional order β is too small, the integration effect may lead to the stable condition $\frac{d\Upsilon(t)}{dt}\le0$ unsatisfied promptly, since $\frac{d\Upsilon(t)}{dt}$ contains the integral term ${}_0D_t^{1-\beta}$

which may induce the phase delay or part variation magnitude of $\frac{d\Upsilon(t)}{dt}$ (more details in [34]). Therefore, the above system will be divergent when the fractional order β is in $(0, 0.4)$. For the fractional order γ of the fractional-order PI controller (26) for spraying control, we note that the fractional order needs to satisfy some certain range to make the tempered anomalous diffusion system stable, which is provided in [35,36] for the general fractional-order system. Although the range of fractional order γ of the fractional-order PI controller (26) for the tempered anomalous diffusion system (10) may not be precisely estimated due to the uncertainty and disturbance of the tempered anomalous diffusion model, it is still reasonable that the above tempered anomalous diffusion system is divergent when the fractional order γ is in $(0, 0.4)$. In this paper, we obtain the suitable range of fractional order of the fractional-order PI controllers for actuators motion and spraying through the numerical simulation.

5.3. Case of moving pollution source

The tempered anomalous diffusion process with a moving pollution source and control input is depicted as the PDE (10), where $f_d(\cdot) = f_{md}(\cdot)$ represents a moving pollution source, control input and boundary conditions are the same as the static scenario.

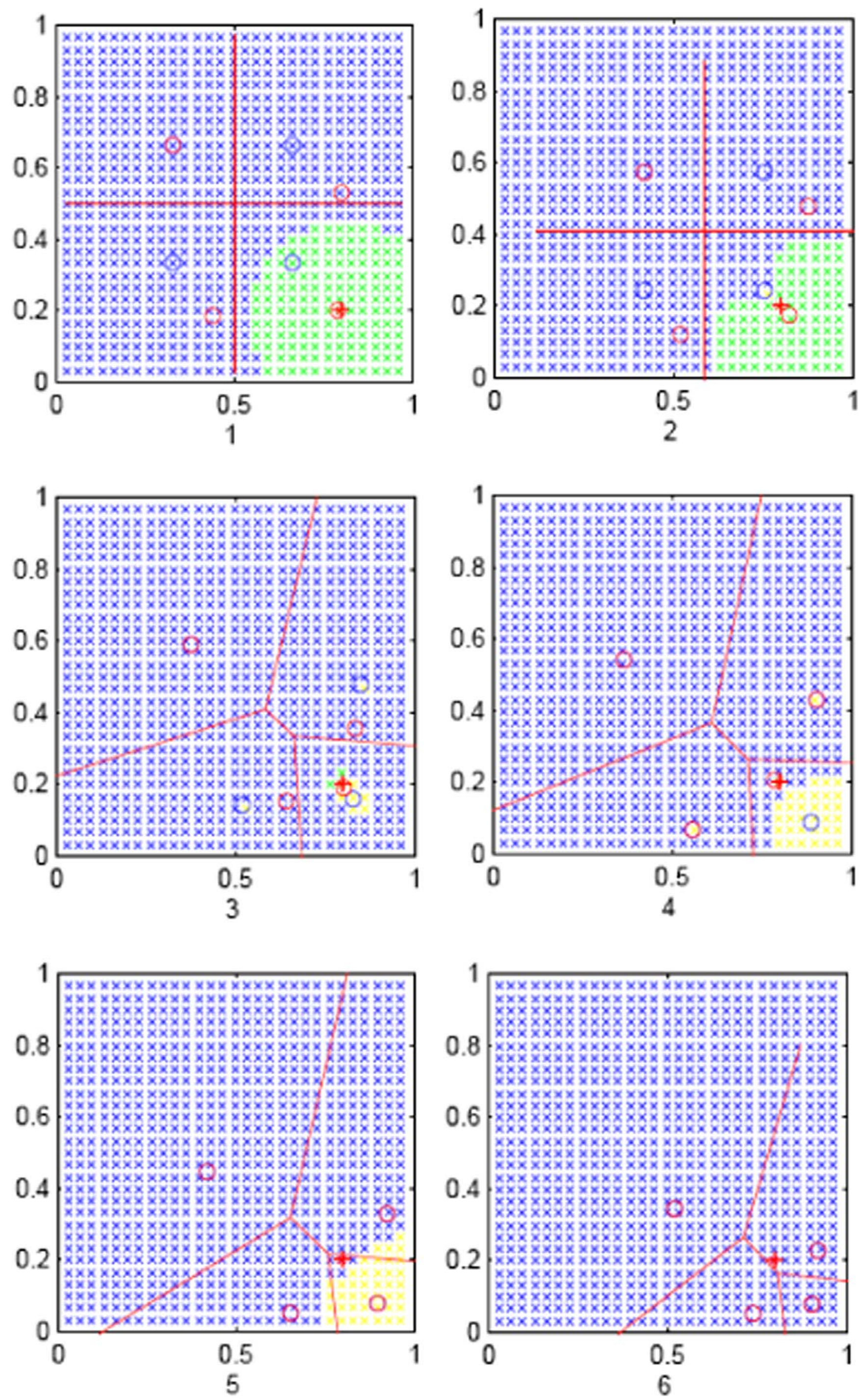

Fig. 3. Movement of mobile actuators when they converge to centroids of Voronoi configurations with a static pollution source. Blue circles represent actuators. Red circles denote centroids (the desired position of actuators). Red polygons are Voronoi cells. The green area represents the pollution combination of space point in current time. The yellow area means the actuator sprays too much in this area at the current time.

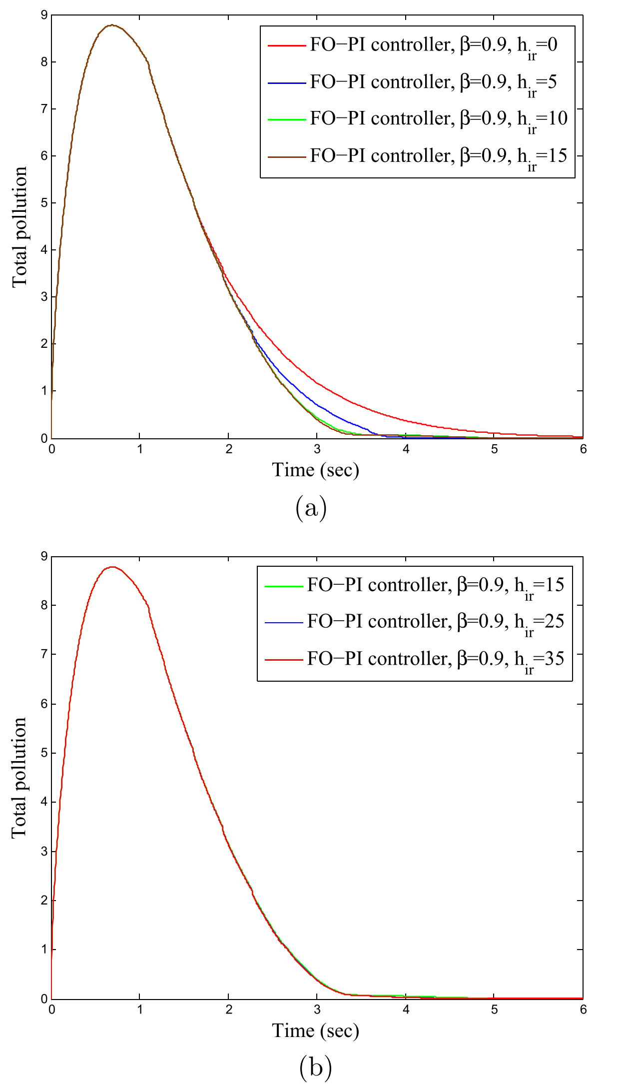

Fig. 4. Evolution of total pollution amount with different value of h_{ir} for spraying control of a static pollution source.

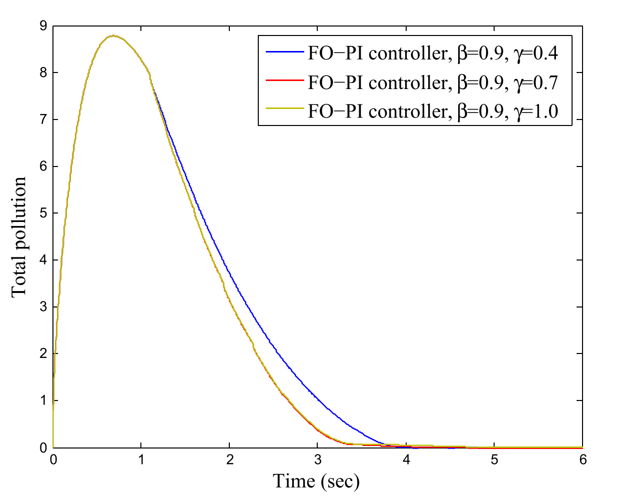

Fig. 5. Variation of total pollutant with different value of γ for spraying control of a static pollution source.

The moving disturbance source is taken as a point disturbance $f_{md}(\cdot)$ to the tempered anomalous diffusion process, whose moving trajectory is given by

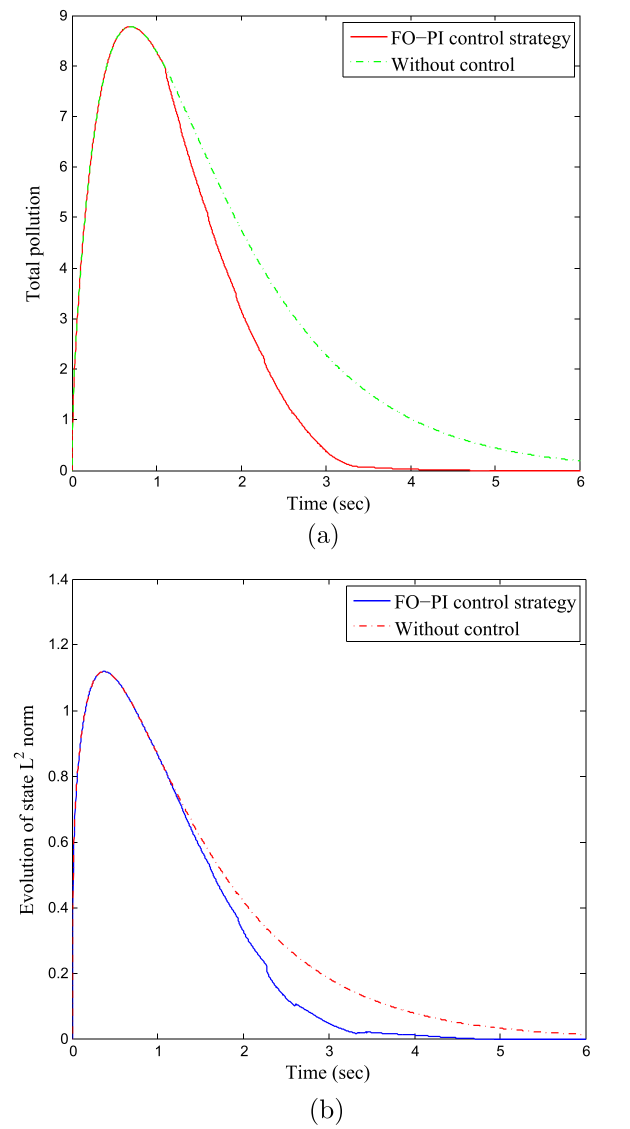

Fig. 6. Evolution of the pollution amount and state L_2 norm under the fractional-order PI control strategy and without control of a static pollution source.

Table 1
Evolution of pollution amount and state L_2 norm of a static pollution source.

Time (s)	FO-PI control strategy		Without control	
	Amount	Norm	Amount	Norm
1	8.40	0.84	8.40	0.84
2	3.25	0.32	4.80	0.42
3	0.40	0.05	2.30	0.19
4	0.01	0.01	1.00	0.08
5	0.00	0.00	0.45	0.04
6	0.00	0.00	0.20	0.02

$$\begin{cases} x = 0.5 + 0.3\cos(2\pi t/50) \\ y = 0.2 + 0.3\sin(2\pi t/50)' \end{cases} \tag{29}$$

and the moving pollution source equation is represented as below

$$f_{md}(t) = 20e^{-t}\Big|_{(x=0.5+0.3\cos(2\pi t/50),y=0.2+0.3\sin(2\pi t/50))}. \tag{30}$$

First, the proportional coefficient h_p, the viscous coefficient h_v and the integral coefficient h_i are given by 9, 1, 1, respectively. For

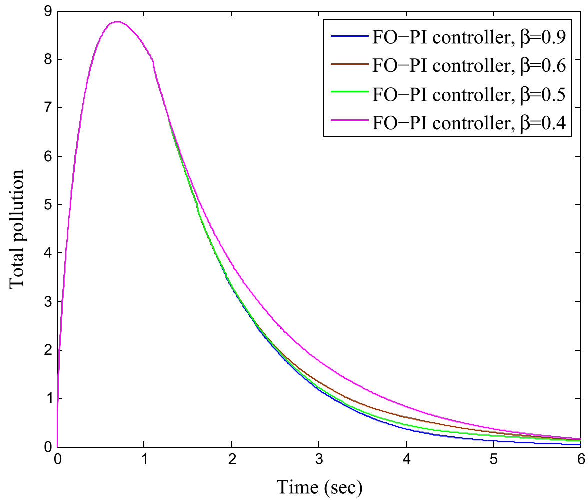

Fig. 7. Evolution of total pollution amount according to different value of β for actuator motion control of a moving pollution source.

obtaining the optimal fractional order β of (20), we let β vary from 0.4 to 0.9 in Fig. 7. From the simulation results, we can find that the total pollutant has got to the lowest at the end of simulation time at $\beta = 0.9$ in Fig. 7. It is necessary to point out the second-order dynamic system (21) is divergent when $\beta < 0.4$ for each actuator (see Remark 5, 6 for more details). Then, according to the optimal fractional order β, it is obvious that we can obtain the control input equation for actuator motion as follows

$$u_{l_i} = 9\left(\bar{l}_i - l_i\right) + {}_0D_t^{-0.9}\left(\bar{l}_i - l_i\right) - \dot{l}_i. \tag{31}$$

In spraying control process, we let the proportional coefficient $h_{pr} = 10$, the integral coefficient h_{ir} varying from 0 to 30 with the step 5 and 10, which are shown in Fig. 8(a) and (b), respectively. With the same explanation as the static issue, we take $h_{ir} = 10$ in our following simulations. In order to get the total pollutant lower as soon as possible, we choose the optimal time fractional order γ of (26) from 0.4 to 1.0. From the simulation results in Fig. 9, it is easy to obtain that the optimal fractional order γ is 0.5. In addition, for $\gamma < 0.4$, the tempered anomalous diffusion system (10) with a moving source is also divergent as in the case of the static pollution source (see Remark 5, 6 for more details). Moreover, the spraying control input can be taken as

$$u_{s_i}(t) = -10\bar{\varphi}_i(x, y, t) - 10\,{}_0D_t^{-0.5}\bar{\varphi}_i(x, y, \tau). \tag{32}$$

From Fig. 10, we can find that the pollution amount and state L_2 norm under the fractional-order control force fall faster than the counterpart with no control input to exert. In addition, Table 2 implies that the amount of total pollution decreases to zero after $t = 5\,s$ and the state L_2 norm falls to zero completely under the fractional-order PI controllers, while the counterpart approaches to the approximate values 0.2 and 0.01 without control at last, respectively. They both verify the validity of our proposed control method.

Remark 6. In the case of moving pollution source, the fractional orders β and γ of the fractional-order PI controllers for actuators motion control and spraying control are also not in some certain range $(0, 0.4)$ to make the actuator's second dynamic system (21) and the tempered anomalous diffusion system (10) stable, whose

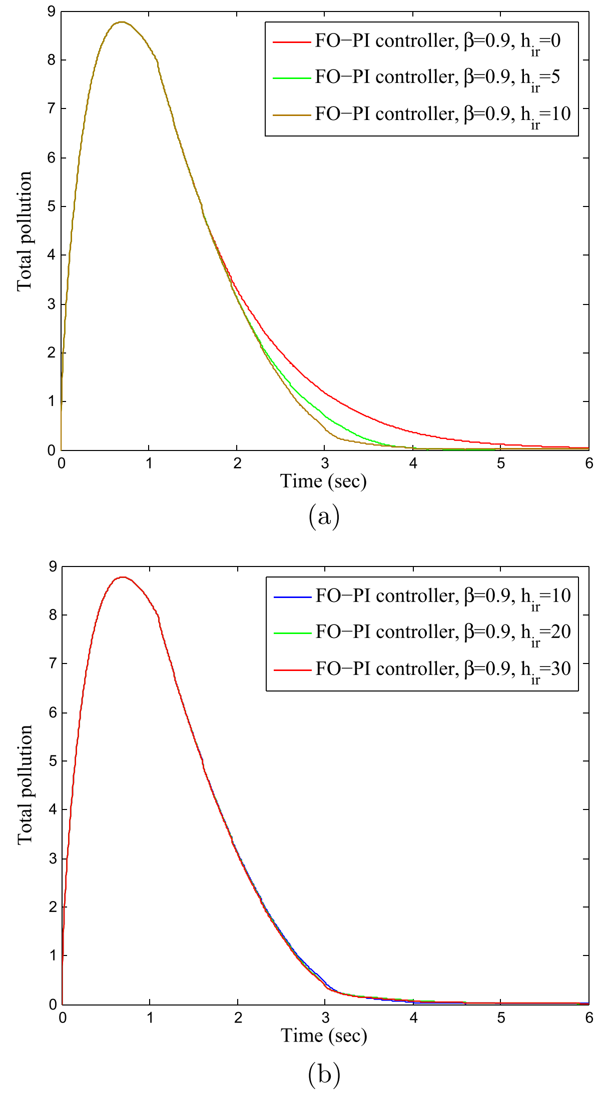

Fig. 8. Evolution of total pollution amount with different value of h_{ir} for spraying control of a moving pollution source.

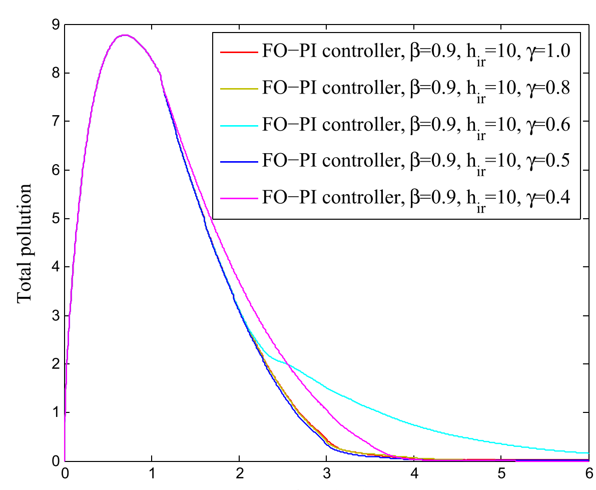

Fig. 9. Variation of total pollutant with different value of γ for spraying control of a moving pollution source.

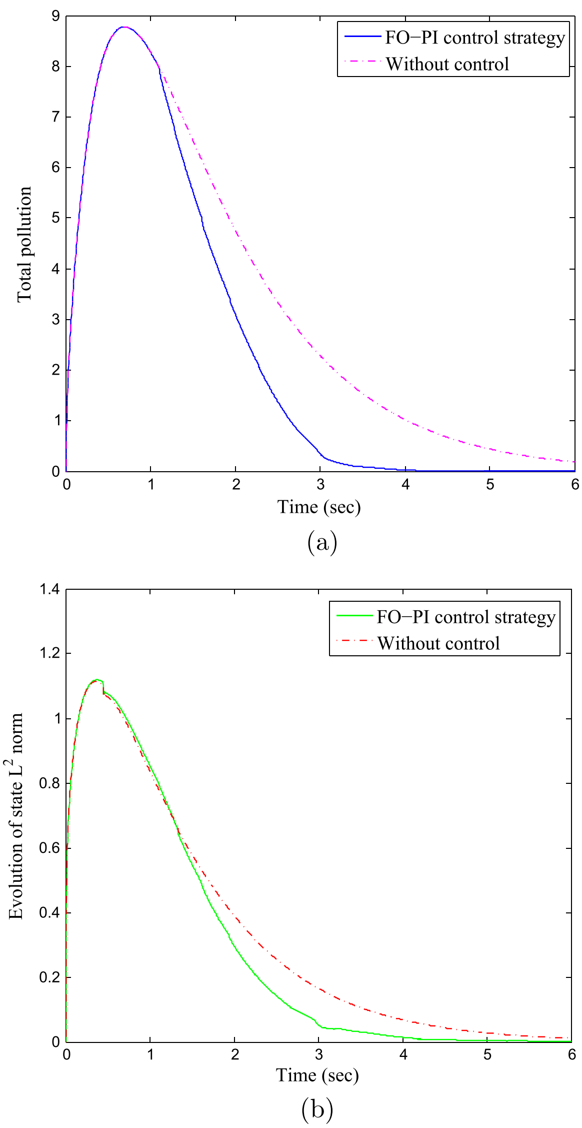

Fig. 10. Evolution of the pollution amount and state L_2 norm under the fractional-order PI control strategy and without control of a moving pollution source.

Table 2
Evolution of pollution amount and state L_2 norm of a moving pollution source.

Time (s)	FO-PI control strategy		Without control	
	Amount	Norm	Amount	Norm
1	8.40	0.84	8.40	0.84
2	3.20	0.26	5.00	0.40
3	0.40	0.08	2.20	0.16
4	0.01	0.01	1.10	0.08
5	0.00	0.00	0.45	0.02
6	0.00	0.00	0.20	0.01

explanation and analytic reason is same as the counterpart of the static issue.

6. Conclusions and future work

This paper investigated diffusion control problem of the tempered anomalous diffusion system by the fractional-order PI controllers for actuator motion and neutralization control. Based on Lyapunov stability arguments, stability of the actuators second-order dynamic system was proved, which illustrated that the control input can achieve convergence of the actuators location to the centroid of Voronoi cells. By designing a fractional-order PI controller, the spraying control problem statement was provided. Finally, utilizing FO-Diff-MAS2D-FOPI simulation platform, two numerical experiments with static and moving pollution sources were presented, which indicated that the fractional-order PI control method could be valid to control the tempered anomalous diffusion process. Namely, improvement with respect to integer-order PI controllers was not clearly obtained. A deeper analysis on advantage of the fractional-order controllers compared with the integer-order controllers for the tempered anomalous diffusion system will be investigated in future work.

Acknowledgements

The authors thank to Dr. Xuyang Lou and reviewers. This work is partially supported by National Natural Science Foundation of China (61174021, 61473136), the Fundamental Research Funds for the Central Universities (JUSRP51322B), the 111 Project (B12018) and Jiangsu Innovation Program for Graduates (Project No. KYLX15_1167 and KYLX15_1170).

References

[1] Khanafer K, Vafai K, Kangarlu A. Water diffusion in biomedical systems as related to magnetic resonance imaging. Magn Resonance Imag 2003;21(1):17–31.
[2] Gerisch A, Chaplain MA. Robust numerical methods for taxis-diffusion-reaction systems: applications to biomedical problems. Math Comput Model 2006;43(1-2):49–75.
[3] Baeumer B, Meerschaert MM. Tempered stable Lévy motion and transient super-diffusion. J Comput Appl Math 2010;233(10):2438–48.
[4] Gajda J, Magdziarz M. Fractional Fokker-Planck equation with tempered α-stable waiting times: Langevin picture and computer simulation. Phys Rev E 2010;82(1):011117.
[5] Li C, Deng WH, Zhao LJ. Well-posedness and numerical algorithm for the tempered fractional ordinary differential equations, arXiv:arxiv:1501.00376; 2015.
[6] Sabzikar F, Meerschaert MM, Chen J. Tempered fractional calculus. J Comput Phys 2015;293:14–28.
[7] Carr P, Geman H, Madan DB, Yor M. Stochastic volatility for Lévy processes. Math Financ 2003;13(3):345–82.
[8] Cartea A, del Castillo-Negrete D. Fractional diffusion models of option prices in markets with jumps. Phys A: Stat Mech Appl 2007;374(2):749–63.
[9] Meerschaert MM, Zhang Y, Baeumer B. Tempered anomalous diffusion in heterogeneous systems. Geophys Res Lett 2008;35(17):L17403.
[10] Meerschaert MM, Sabzikar F, Phanikumar MS, Zeleke A. Tempered fractional time series model for turbulence in geophysical flows. J Stat Mech: Theory Exp 2014;2014(9):P09023.
[11] Du Q, Faber V, Gunzburger M. Centroidal Voronoi tessellations: applications and algorithms. SIAM Rev 1999;41(4):637–76.
[12] Cortés J, Martínez S, Karatas T, Bullo F. Coverage control for mobile sensing networks. IEEE Trans Robot Autom 2004;20(2):243–55.
[13] Chen YQ, Moore KL, Song Z. Diffusion boundary determination and zone control via mobile actuator-sensor networks (MAS-net): challenges and opportunities. In: Proceedings of SPIE conference on intelligent computing: theory and applications II, part of SPIE's defense and security; 2004. p.102–13.
[14] Stark B, Rider S, Chen YQ. Optimal control of a diffusion process using networked unmanned aerial systems with smart health. IFAC Proceedings Volumes 2014;47(3):1254–9.
[15] Ju LL, Du Q, Gunzburger M. Probabilistic methods for centroidal voronoi tessellations and their parallel implementations. Parallel Comput 2002;28(10):1477–500.
[16] Chen YQ, Wang ZM, Liang JS. Optimal dynamic actuator location in distributed feedback control of a diffusion process. In: Proceedings of the 44th IEEE conference on decision and control and the European control conference; 2005. p. 5562–7.
[17] Cao JX, Chen YQ, Li CP. Multi-UAV-based optimal crop-dusting of anomalously diffusing infestation of crops, ⟨http://arxiv.org/abs/1411.2880v3⟩; 2014.
[18] Chen YQ. Ubiquitous fractional order controls. IFAC Proceedings Volumes 2006;39(11):481–92.
[19] Podlubny I. Fractional-order systems and $PI^{\lambda}D^{\mu}$-controllers. IEEE Trans Autom Control 1999;44(1):208–14.
[20] Outsaloup A. La Commande CRONE: Commande Robuste d'Ordre Non Entiére, Paris, France: Hermes; 1991.

Please cite this article as: Juan Chen, et al. Diffusion control for a tempered anomalous diffusion system using fractional-order PI controllers. ISA Transactions (2017), http://dx.doi.org/10.1016/j.isatra.2017.04.005

[21] Chen YQ, Ahn H-S, Podlubny I. Robust stability check of fractional order linear time invariant systems with interval uncertainties. Signal Process 2006;86 (10):2611–8.
[22] Ahn H-S, Chen YQ, Podlubny I. Robust stability test of a class of linear time-invariant interval fractional-order system using Lyapunov inequality. Appl Math Comput 2007;187(1):27–34.
[23] Özdemir N, Iskender BB. Fractional PI $^{\lambda}$ controller for fractional order linear system with input hysteresis, In: Proceedings of European nonlinear oscillations conferences, Saint Petersburg, Russia; 2008.
[24] Ge FD, Chen J, Chen YQ, Kou CH. Optimal spraying control of a tempered time fractional order anomalous diffusion system, In: Proceedings of the international symposium on fractional signals and systems, Romania; 2015, p. 43–8.
[25] Li Y, Chen YQ, Podlubny I. Stability of fractional-order nonlinear dynamic systems: Lyapunov direct method and generalized Mittag-Leffler stability. Comput Math Appl 2010;59(5):1810–21.
[26] Liang JS, Chen YQ. Diff-MAS2D (version 0.9) user's manual: A simulation platform for controlling distributed parameter systems (diffusion) with networked movable actuators and sensors (MAS) in 2D domain, Tech. Rep. USU-CSOIS-TR-04-03, CSOIS,Utah State University; 2004.
[27] Podlubny I. Fractional differential equations: an introduction to fractional derivatives, fractional differential equations, to methods of their solution and some of their applications. San Diego, CA: Academic Press; 1998.
[28] Samko SG, Kilbas AA, Marichev OI. Fractional integrals and derivatives: theory and applications. Philadelphia, Pa., USA: Gordon and Breach Science Publishers;1993.
[29] Howard, A, Matarić MJ, Sukhatme GS. Mobile sensor network deployment using potential fields: A distributed, scalable solution to the area coverage problem, In: Proceedings of the 6th international symposium on distributed autonomous robotic systems (DARS02), Fukuoka; 2002. p. 299–308.
[30] Van der Schaft A. L_2-gain and passivity techniques in nonlinear control. 2nd Edition. New York: Springer- Verlag; 1999.
[31] Efe MÖ. ADALINE based robust control in robotics: a Riemann-Liouville fractional differintegration based learning scheme. Soft Comput 2009;13(1):23–9.
[32] Chao HY, Chen YQ. Remote sensing and actuation using unmanned vehicles, 3. Hoboken, NJ, USA: John Wiley & Sons; 2012.
[33] Xue DY, Chen Y. System simulation techniques with MATLAB and simulink. New Jersey, USA: Wiley & Sons; 2013.
[34] Huang JC, Li HS, Chen YQ, Xu QH. Robust position control of PMSM using fractional-order sliding mode controller. Abstr Appl Anal 2012:1–33.
[35] Petrávs I. Stability of Fractional-Order Systems, Berlin Heidelberg: Springer-Verlag, 2011.
[36] Hamamci SE. Stabilization using fractional-order PI and PID controllers. Nonlinear Dyn 2008;51(1):329–43.

Please cite this article as: Juan Chen, et al. Diffusion control for a tempered anomalous diffusion system using fractional-order PI controllers. ISA Transactions (2017), http://dx.doi.org/10.1016/j.isatra.2017.04.005